Ion Dynamics and Velocities in Titan's Upper Atmosphere

J. H. Westlake[1*], V. L. Toy-Edens[1], A. J. McCubbin[1]

[1]Johns Hopkins University Applied Physics Laboratory, 11000 Johns Hopkins Rd. Laurel, MD 20723

Key Points:

- Cassini measurements show heavy atmospheric ions being accelerated in Titan's upper atmosphere
- Several Cassini flybys show a direct connection from the thermal atmospheric ions to the suprathermal and accelerated ion components
- Multiple ion acceleration processes are likely at play with some being mass dependent and some being mass independent

*11000 Johns Hopkins Rd., Laurel, MD 20723

Corresponding author: Joseph Westlake, `joseph.westlake@jhuapl.edu`

Abstract

The Cassini mission yielded a treasure trove of information on Saturn's largest moon Titan. With many flybys of this complex moon Cassini revealed many aspects of Titan's upper atmosphere and interaction with Saturn's magnetosphere. In many ways Cassini revealed that this moon is unique in that it sustains a dense atmosphere and ionosphere even without the protection of an internal magnetic field. Key to the understanding of this ionosphere is understanding the ion dynamics of Titan's upper atmosphere, namely how these ions are created and lost either to the lower atmosphere where they fall and can contribute to the creation of the complex hydrocarbons seen at the surface or are carried away with Saturn's rapidly flowing magnetospheric particles. Here we present novel measurements of the velocities of many ion species in Titan's upper atmosphere. We show that multiple processes must be responsible for the acceleration of these ions as there is evidence for both mass dependent and independent acceleration. We also show that heavy, relatively complex molecular ions are accelerated and carried into the magnetospheric flow. These ions could contribute to mass loading processes and possibly additional changes in the magnetosphere when Titan resides in Saturn's magnetotail.

Plain Language Summary

Titan's complex atmosphere produces many hydrocarbon species at high altitude. These hydrocarbons must either sink to the lower atmosphere and eventually the surface or be carried away with the particles that are trapped in Saturn's rapidly rotating magnetic field. We show that some of these large hydrocarbons are carried away from Titan as ions.

1 Introduction

The moons of the giant planets in our solar system each have unique interactions with their parent bodies' magnetosphere. The giant planets produce expansive magnetospheres that rapidly rotate resulting in substantial flows of fast-moving plasma over their moons. The interaction of Saturn's magnetosphere with Titan's upper atmosphere is a complex interaction of rapidly flowing plasma that has been sourced and accelerated closer to the planet with the complex hydrocarbon ionosphere of Titan. This interaction sets up an induced magnetosphere that serves as an obstacle for the rapidly flowing magnetospheric plasma. The transfer of energy from the magnetosphere into the atmosphere either through acceleration or heating processes is of interest across the solar system where many moon-magnetosphere interactions exist.

The Voyager and Cassini spacecraft have studied Titan's moon-magnetosphere interaction. Voyager flew through Titan's tail in a single pass finding a dual lobed structure with light ions dominating one lobe and heavy ions dominating the other (Hartle et al., 1982; Sittler et al., 2005). Cassini repeatedly visited Titan's ionosphere, extended atmosphere, and tail regions in a multitude of geometries revealing that the interaction of Titan's ionosphere with Saturn's magnetosphere is much more complex than the simple picture from the Voyager flyby (e.g., Westlake et al. (2016)).

Many simulations of the interaction of Titan's extended atmosphere with Saturn's magnetosphere have been produced for various studies. Of note for this investigation are the models which include not just the photochemical production and loss of ionospheric particles within the main ionosphere, but models that look at the transport of ions. Early MHD modeling of the interaction along with simple photochemistry showed that above about 1400 km in altitude the photochemical lifetimes of the ions became long with respect to the transport timelines (Cravens et al., 1998; Ma et al., 2004). At this crucial and complex transition from a photochemically dominated ionosphere to a transport dominated exosphere the composition of the ions becomes much more static. The low densities reduce the incidence of ion-neutral reactions and electron recombination. However, transport processes tend to favor light ions because momentum transfer can be much more efficient. Therefore, in assessing the global atmospheric escape the question has always been over how light species like molecular hydrogen and methane escape (Bell et al., 2014; Strobel, 2009).

With charged particles from the ionosphere however it is possible to lift much heavier particles and propel them into Saturn's magnetosphere due to the many additional electromagnetic forces at play. The relative quantities of material that can be expelled into space is dominated by the neutral atmosphere. However, the ionosphere may be the place where complex hydrocarbons can be sourced and eventually transported further in the Saturn system having implications for chemistry throughout the system. Many studies have attempted to attain an estimate of the escape rate of ions from Titan yielding estimates in the $10^{24} s^{-1}$ to $10^{25} s^{-1}$ range (Jiang et al., 2019; Regoli et al., 2016; Romanelli et al., 2014) and while the quantity of ions escaping from Titan is important, it is also important whether these ions are compositionally complex or simple photochemical products of the primary neutral molecules H_2, CH_4, and N_2.

In this study we detail multiple specially planned observations of the Cassini Ion and Neutral Mass Spectrometer (INMS) instrument (Waite et al., 2004) and derive ion velocities using the Cassini Plasma Spectrometer Ion Beam Sensor (CAPS-IBS) instrument (Young et al., 1996) to observe the first steps in acceleration of ions from Titan's ionosphere. Specifically, we show that both mass-dependent and mass-independent acceleration is observed indicating that the outflow of ions likely has multiple processes at work, some of which are capable of propelling heavy ions from Titan's ionosphere into Saturn's magnetosphere.

2 Observations

In this study we make use of observations made on different Titan flybys from the Cassini INMS and CAPS-IBS instruments. Both instruments produced a plethora of measurements throughout the Cassini mission, however due to the nature of the mission and the pointing requirements to get quality ion measurements only a few flybys were dedicated to INMS or CAPS measurements and even fewer were dedicated to producing the ion measurements which required dedicated pointing for INMS and CAPS. In this section we detail the measurement techniques and datasets that we utilize for this study.

2.1 INMS Ion Velocity Measurements

The INMS instrument can only measure velocities along the direction of motion of the spacecraft. For the study of along-track velocities as measured by INMS we focus on a trio of special observations made during the T95 (14 October 2013), T00 (7 April 2014), and T113 (28 September 2015) Titan flybys with geometries shown in Figure 1. The INMS instrument measures ionized and neutral particles using a quadrupole mass spectrometer. Ions and neutrals with thermal velocities significantly less than the spacecraft velocity (6 km/s) form a high-Mach beam into the INMS open source. Ions enter the instrument through the quadrupole switching lens (QSL) that focus the beam and bends it through 90° into the quadrupole mass analyzer. The voltages on the QSL are tuned to specific velocities of incoming ions using both on the ground calibrations (Waite et al., 2004) and in-space calibrations (Mandt et al., 2012). The QSL acts as an electrostatic analyzer for the incoming ions, and while not originally intended for this purpose, we were able to produce, late in the Cassini mission, an operational mode that scanned the QSL voltages to retrieve a representative velocity distribution of the thermal ions. The ability to use the QSL as an electrostatic analyzer was intended to be able to tune the incoming beam to maximize the sensitivity of INMS, however during the prime mission it was used more of a check to determine the rough sensitivity of the instrument.

Westlake et al. (2012) discovered that when there is a mismatch in the settings of the intended QSL voltages and the spacecraft velocity along with an abundance of suprathermal or accelerated ions the INMS instrument can directly observe ions that are flowing away from Titan. The special QSL operation step over several voltage values to scan the incoming beam keeping the selected mass in the quadrupole mass analyzer constant to obtain velocity distributions for several ion species, specifically we chose to look for ions with masses of 2, 15, 16, 17, 28, 29, and 39. The choice of ion masses contains contributions from very light ions (H_2^+) as well those in the first, second, and third hydrocarbon group with the goal of being able to assess the acceleration processes at work using the differences in the velocity distributions for these masses.

The first attempted custom QSL table observation from the INMS occurred during the T86 flyby (26 September 2012). During this flyby the INMS voltages were swept across a wide range in an exploratory fashion. This flyby retrieved data indicating that there are cold beams that are accelerated away from Titan, however the settings didn't retrieve useful or complete velocity distributions. The T86 experience was used to refine the QSL voltage tables for future flybys and will not be discussed further in this work other than to note that mass 2 was not observed in any substantial quantities even though it was swept over a much larger energy range during this flyby. We note that the lack of mass 2 in the observations is not likely due to the lack of substantial quantities of H_2^+ in Titan's exosphere but due to the instruments' inability to observe these ions due to lack of velocity space coverage in the INMS power supply capabilities. In general, previous studies of ions in Titan's upper atmosphere have strayed from making conclusions on light ions due to this concern, which we will revisit when discussing the CAPS-IBS measurements which have a much broader energy range. With the data from the T86 flyby the INMS team revised the INMS voltage settings to narrow in on the expected ion velocities resulting in the parameters shown in Figure 2.

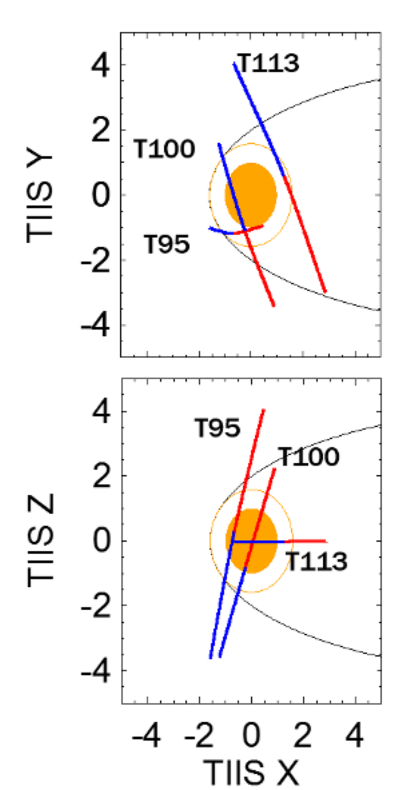

Figure 1. The geometry of the T95, T100, and T113 flybys in Titan interaction system (TIIS) coordinates. The red indicates the ingress portion of the flyby, and the blue is the egress portion of the flyby. Also plotted is a notional shape for the Titan interaction that is simply placed to indicate the magnetospheric flow direction as from the negative TIIS X to positive TIIS X direction. Saturn is in the negative Y direction and Z completes the right-handed system.

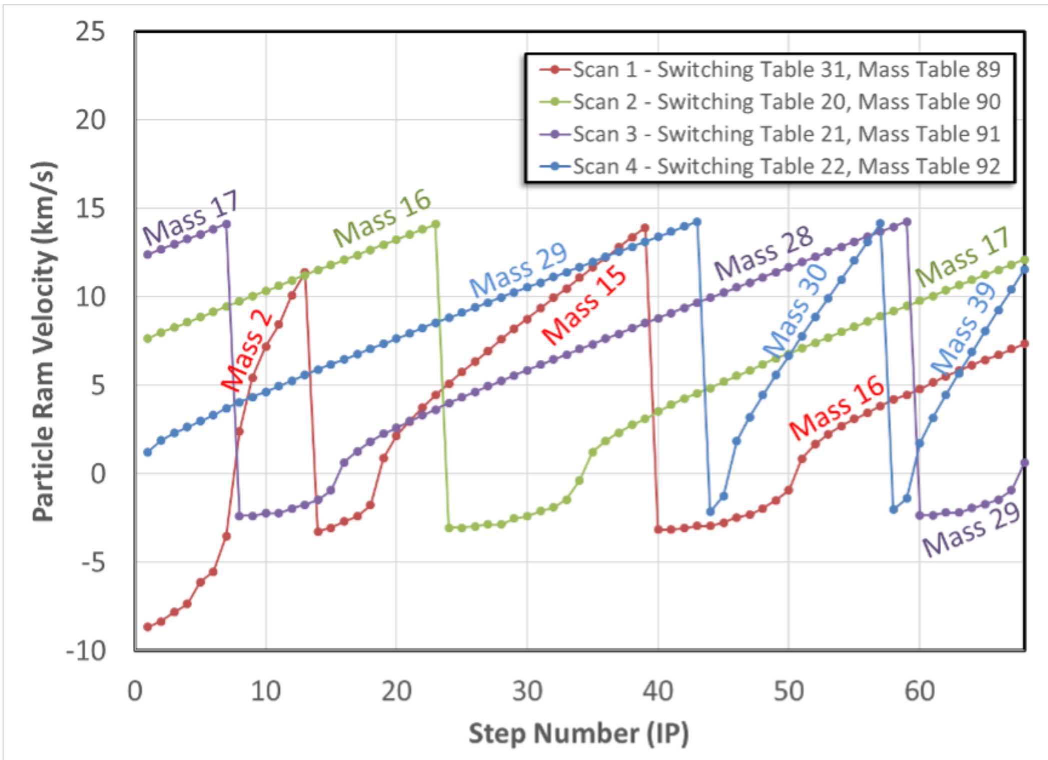

Figure 2. The stepping sequence used by the INMS during ionospheric observations. The sequence consisted of four scans containing internal voltages that produce the velocity scans shown above. The mass numbers shown represent the settings of the mass selecting quadrupole during that portion of the sweep. The velocities given are the nominal ram velocities assuming no spacecraft potential and velocities direct into the ram direction. The masses were selected to capture many of the primary ions from Titan's ionosphere as well as some trace ions that are produced lower in the ionosphere.

The T95 (ingress and egress), T100 (ingress), and T113 (egress) flybys showed unique features in their velocity distributions for these ions. The velocity distributions are shown in Figures 3, 4, and 5. For each figure we show the ion velocity that is derived from the quadrupole lens voltage settings in the same way as was done by Mandt et al. (2012). These figures display for each mass a velocity distribution plotted versus the counts observed in the instrument. Each measurement is obtained with the same sampling time, so pure counts is acceptable. We note that because this mode was never planned for the INMS the retrieval of densities or even fluxes into the instrument was not attempted due to a lack of calibration for this mode, however comparing the relative counts at each voltage setting does give a rough idea of the velocity distribution for each mass. Each point and line are colored with the mean altitude of the scan and generally ranges from about 1400 km to nearly 2500 km.

As expected for Titan's ionosphere the density of ions is generally observed to increase with decreasing altitude for the altitudes sampled here. The velocity measurement presented here is purely the along-track component of the velocity and gives no indication of what the cross-track velocity is. For the INMS observations we have no additional information about the direction of the ion flows so we utilize the Gaussian nature of the velocity distribution to obtain useful fiduciaries, namely the mean velocity and distribution width, which could be associated with the temperature of the distribution. We do this for masses 15, 16, 17, 28, 29, and 30. Due to constraints on the observations the number of measurements within the velocity distributions for mass 30 and mass 39 were reduced in favor of higher resolution velocity distributions for the lower mass ions. The central velocities have the spacecraft velocity subtracted such that they give the ambient measured velocity along the direction of travel of Cassini.

We show the derived central velocities versus altitude along with the Langmuir Probe derived spacecraft potential for the T95, T100, and T113 flybys in Figure 6. We plot the spacecraft potential to look for periods where significant offsets in the measured velocity would be expected from acceleration to a charged spacecraft. We note that Cassini regularly became charged in Titan's upper atmosphere and exosphere, however below about 2000 km Cassini would generally charge to about -1 V. We note that none of the spacecraft potentials shown in Figure 6 show clear relations with the accelerations observed.

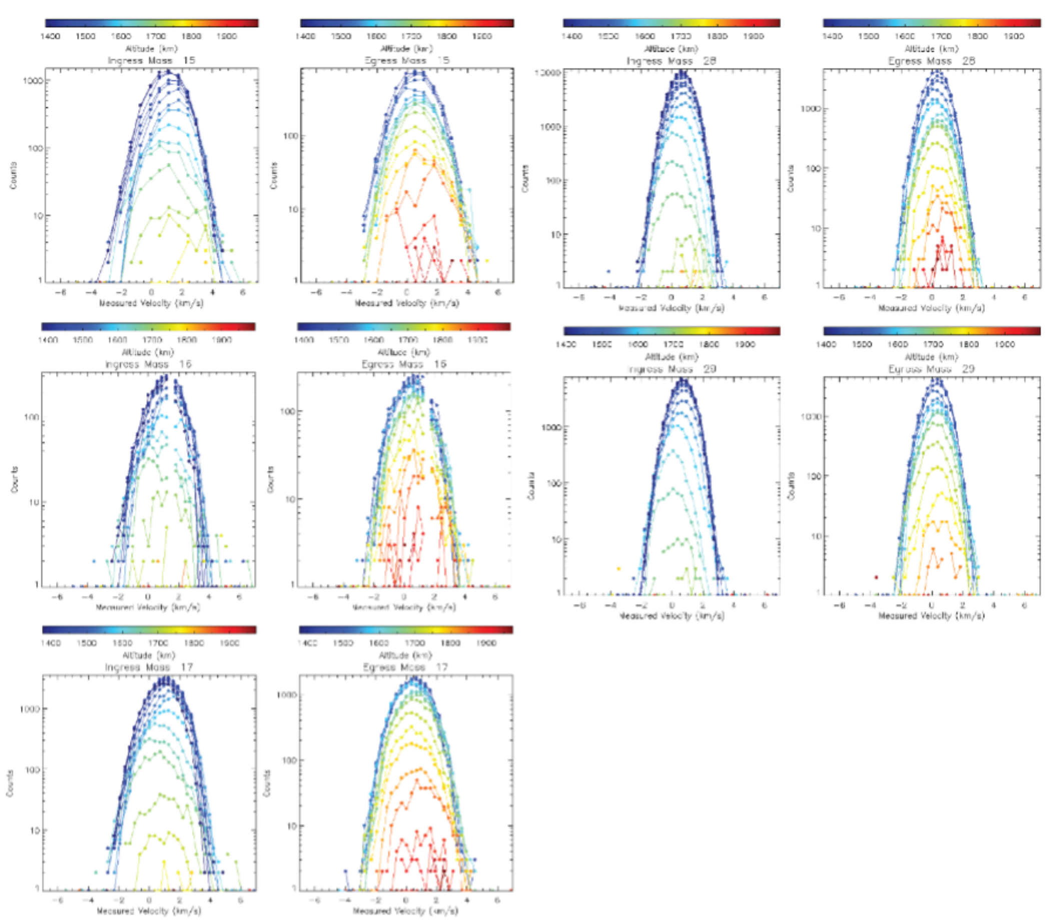

Figure 3. Velocity distributions of Titan's topside ionospheric ions during the T95 flyby. Each plot corresponds to a specific mass and segment of the flyby (ingress or egress). The plots correspond to masses 15, 16, 17, 28, and 29. The coloring of each point corresponds to the altitude that the measurement was taken.

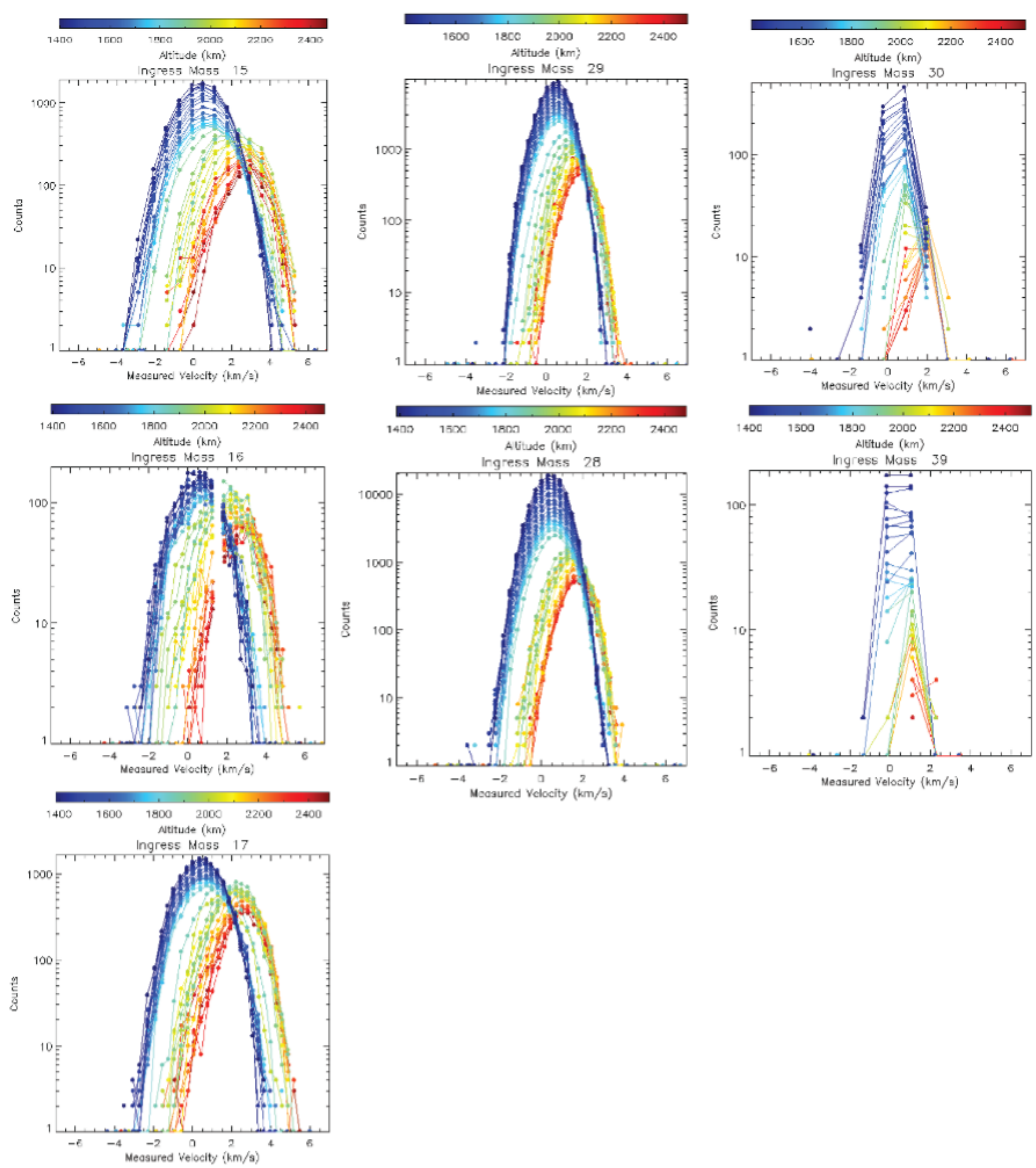

Figure 4. Same as Figure 3 but for the ingress portion of the T100 flyby for masses 15, 16, 17, 28, 29, 30, and 39.

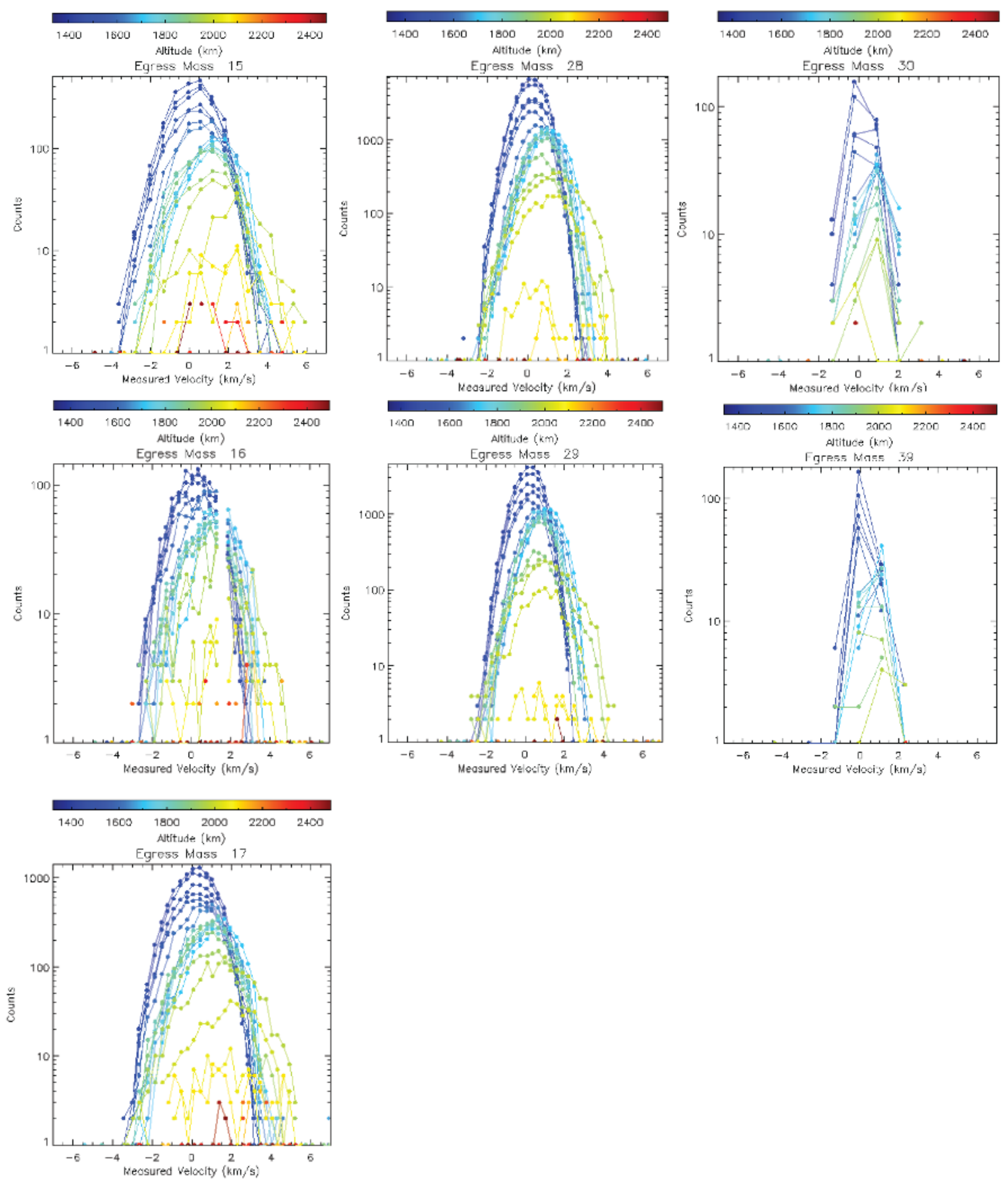

Figure 5. Same as Figure 3 but for the egress portion of the T113 flyby for masses 15, 16, 17, 28, 29, 30, and 39.

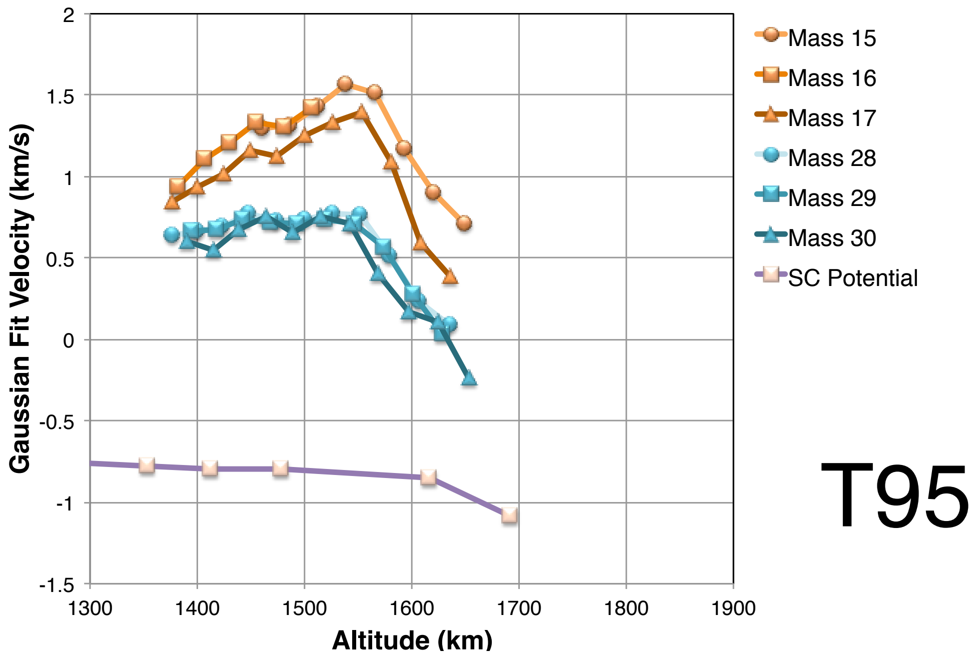

Gaussian Fit Velocity (km/s)
Altitude (km)
Mass 15
Mass 16
Mass 17
Mass 28
Mass 29
Mass 30
SC Potential
T95

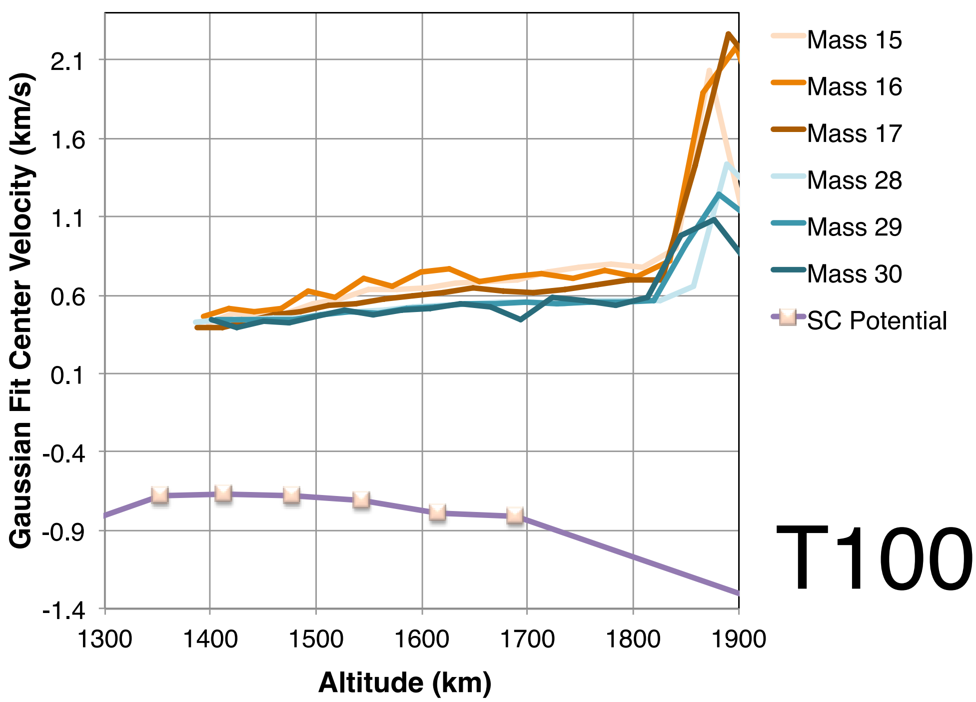

Gaussian Fit Center Velocity (km/s)
Altitude (km)
Mass 15
Mass 16
Mass 17
Mass 28
Mass 29
Mass 30
SC Potential
T100

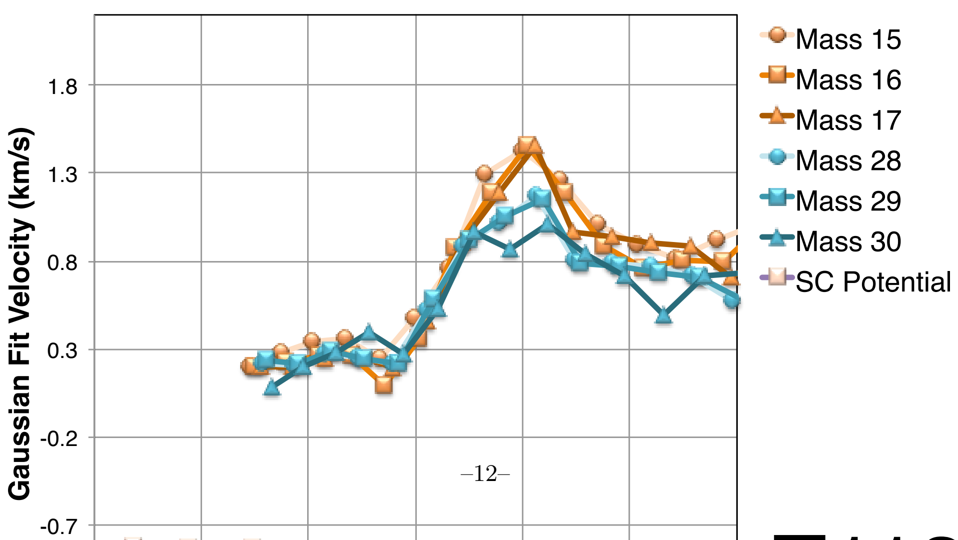

Gaussian Fit Velocity (km/s)
Mass 15
Mass 16
Mass 17
Mass 28
Mass 29
Mass 30
SC Potential

All three flybys show relatively benign velocities of a few hundred m/s up to about 3 km/s with some fairly significant changes versus altitude. Because of the nature of the INMS observation we cannot tell whether these changes are pure accelerations or changes in direction of the flow, however because we are measuring multiple species at the same time we can see how these changes in velocity affect the different species.

During the T95 flyby, which is a north to south flyby the inbound portion shows a distinct increase in velocity from 1650 km to 1550 km with the lighter species having a greater velocity change than the heavier ions. On the outbound portion the results are much more mixed with a wider range of velocities and no clear mass dependence. Although if we interpret mass 16 and 17 as being distinct from mass 28 and 30 they clearly show differences in velocities while masses 15 and 29 appear to have the same velocity throughout. Mass 15 is generally associated with CH_3^+ and mass 29 is associated with $C_2H_5^+$ (e.g. Vuitton et al. (2008)) both of which are rapidly produced byproducts of photolysis of methane.

The T100 flyby shows clear acceleration at the higher altitudes with a distinct separation in mass. Below 1850 km the velocities between the light and heavy ions is nearly identical with the lighter species showing slightly greater velocities than the heavier ones. Above 1850 km there is a clear and distinct increase in observed velocity with the group of light ions showing velocities up to 3 km/s above 2300 km. T100 has a similar flyby geometry to T95 in that it is primarily a north to south flyby.

T113 shows a different picture altogether. During this flyby, which is an equatorial flyby across Titan's tail we see a more collective, bulk behavior of the ions with both heavy and light ions showing nearly identical velocities throughout. We see a change in velocity at 1600 km that goes up to 1.3 km/s. In this change in velocity there is a slight difference in the velocities of the light and heavy species that appears to persist to higher altitudes. Perhaps within this region of the interaction there are multiple forces in play.

Another point of interest is the comparison of the width of the velocity distribution retrieved for each species. In general the lower mass species show wider peaks and the higher mass species showing narrower peaks. For an ideal gas lower mass particles will have a greater thermal velocity compared to heavier particles at the same temperature. We expect this to be true in Titan's extended ionosphere as well, however as particles are accelerated from this ideal gas distribution additional forces must be accounted for. For most of these flybys we can see not just a change in the center of the velocity distribution but also some narrowing in the width of the peak with greater altitudes. The narrowing of the peak width isn't significant and may be consistent with a reduced peak width as the signal decreases. This indicates that most of the distribution is being accelerated.

2.2 CAPS-IBS Ion Velocity Measurements

Details of the CAPS instrument suite and the CAPS-IBS can be found in Young et al. (1996). The Cassini Plasma Spectrometer (CAPS) onboard Cassini has measured large positive and negative ions through several flybys of Titan's ionosphere (Coates et al., 2007; Waite et al., 2007; Crary et al., 2009) (Coates et al. 2007, Waite et al. 2007, Crary et al. 2009). The CAPS suite of instruments consists of the Ion Mass Spectrometer (CAPS-IMS), the Ion Beam Spectrometer (CAPS-IBS), and the Electron Spectrometer (CAPS-ELS). The CAPS-IBS has been used for its high energy resolution ($0.014\Delta E/E$) as a rudimentary mass spectrometer to measure heavy ions with masses reported above 250 Da. The CAPS-ELS and CAPS-IMS can be used in the same way with a more crude energy resolution. These two curved plate electrostatic analyzers function as mass spectrometers in the environment of Titan's ionsophere because of the large Mach number of the cold ionospheric ions rammed into the instrument during a pass (Cassini is generally moving around 6 km/s with respect to Titan's atmosphere resulting in a Mach number around 14 for a mass of 100 Da.).

Crary et al. (2009) performed the first study of the CAPS-IBS data within Titan's ionosphere. By comparing the composition observed by CAPS-IBS with that observed by INMS and the energy per charge that each ion group appeared at they were able to determine the excess velocity along the track of the Cassini flybys. The magnitude of the measured along-track velocity component was shown for 14 flybys in this study showed that they vary from about 50-260 m/s but didn't show any clear trends. The measurement of along-track ion velocity is only one component of the true velocity vector of the ions. The CAPS-IBS is also able to determine the 3D characteristics of an ion beam through its three-fan technique. For the case of Titan the spacecraft motion through the ionospheric plasma produces the ion beam.

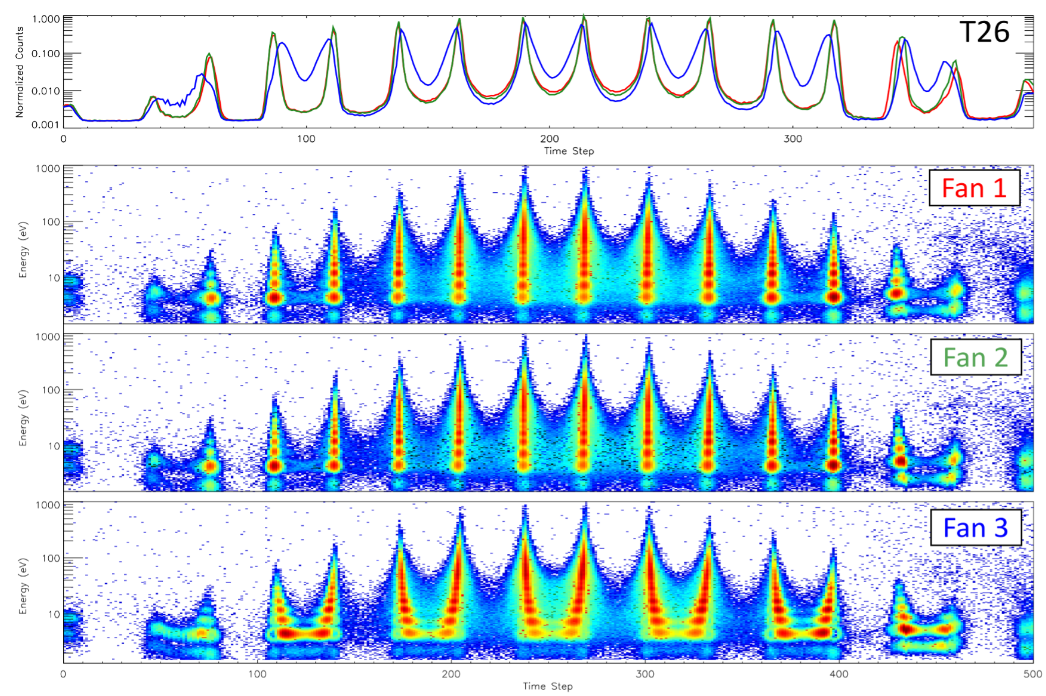

Figure 7. CAPS-IBS Observations from the T26 Titan flyby. The plots show time versus total normalized counts in each fan in the top panel and for the lower three panel energy spectrograms observed by the CAPS-IBS. The CAPS instrument suite is actuating throughout the flyby and observes the signal increase when the field-of-view coincides with the spacecraft ram. The asymmetry in the total count peaks (top panel) about the ram direction indicates a preferred direction of the incoming ions due to ion velocities perpendicular to the spacecraft ram direction.

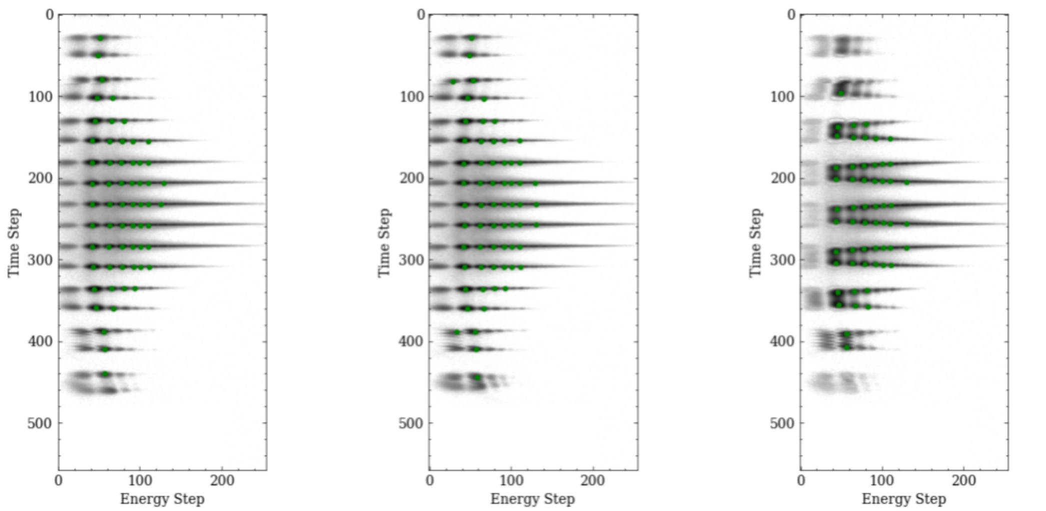

Figure 8. CAPS-IBS Observations from the T40 Titan flyby (5 January 2008). Each panel shows one of the three CAPS-IBS fan's measurements during the flyby. The horizontal axis is the energy step in the instrument and the vertical is a simple time index with the Titan closest approach occurring between time step 200 and 300. Darker colors indicate greater intensities. The green dots show locations where the peak search found local maxima that were used to determine the ion flow velocities.

To obtain the flow direction of an ion beam we utilize the three crossed fan apertures of the CAPS-IBS using a technique used for measuring the solar wind beam described by Bame et al. (1978). Figure 7 shows an example of the data obtained from the CAPS-IBS during the T26 flyby. The CAPS actuator is crucial to this measurement as it sweeps the fans' field of view across the beam and if the actuator angle includes the ram direction of the spacecraft offset by the small velocity change of the ambient ion wind we can measure the direction of that beam. The beam velocity is expected to be composed of two elements, the spacecraft velocity (6 km/s) through the ionosphere and the ion velocities which are expected to be a few 10's to 100's of m/s.

To determine the ion velocities we first determine the actuator angles, α_1, α_2, and α_3 that the peak flux is detected in fans 1, 2, and 3 respectively. Because there are several ions with varying masses we expect that lighter components could have different velocities than the heavier components. We produced a peak searching routine for each flyby to look for the local maxima for each mass grouping. An example of this peak search result is shown in Figure 8.

With the local maxima found in time we can then determine the look direction of each fan from the actuator kernels and from that compose the following vectors normal to the IBS fan-planes

$$\hat{n}_1 = [-cos(30°)cos(\alpha_1), cos(30°)sin(\alpha_1), -sin(30°)] \tag{1}$$

$$\hat{n}_2 = [cos(\alpha_2), sin(\alpha_2), 0] \tag{2}$$

$$\hat{n}_3 = [-cos(-30°)cos(\alpha_3), cos(-30°)sin(\alpha_3), -sin(-30°)] \tag{3}$$

The flow vectors of the ions are then given by taking the cross products between pairs of these vectors.

$$\hat{d}_{12} = \frac{\hat{n}_1 \times \hat{n}_2}{|\hat{n}_1 \times \hat{n}_2|}, \hat{d}_{23} = \frac{\hat{n}_2 \times \hat{n}_3}{|\hat{n}_2 \times \hat{n}_3|}, \hat{d}_{13} = \frac{\hat{n}_1 \times \hat{n}_3}{|\hat{n}_1 \times \hat{n}_3|} \tag{4}$$

Additionally, the flow vectors can be derived using only two of the three fans for the case that one of the fans does not see the peak. Because of the nature of the Titan observations it is common to utilize only two of the three fans for the measurements presented here. This is primarily due to sub-optimal pointing of Cassini for this measurement due to the complex nature of the shared operations across the Cassini payload.

When considering the similar CAPS-IBS measurements of the cross-track ion velocities we see similar features in both the ion velocities and in the relative velocities of the light and heavy ions. Figure 9 shows the cross-track ion velocities using the process described above from several Titan flybys versus altitude as measured by CAPS-IBS.

In analyzing this data we find a similar situation that has plagued the research at Titan from Cassini - the data is very complex without clear structure. The multitude of flybys shown cover a very wide range of conditions at Titan and could indicate any number of different processes at play. However, we can point out a few general trends in the cross-track wind component. First, the cross-track wind component isn't very large with an amplitude of up to 1000 km/s for some rather light species on a few limited observations. Most observations are in the 0-400 m/s range. Therefore, previous observations of along-track winds are consistent with some fairly standard heating processes. Second, the cross-track winds appear to be greater in magnitude for lighter species. This

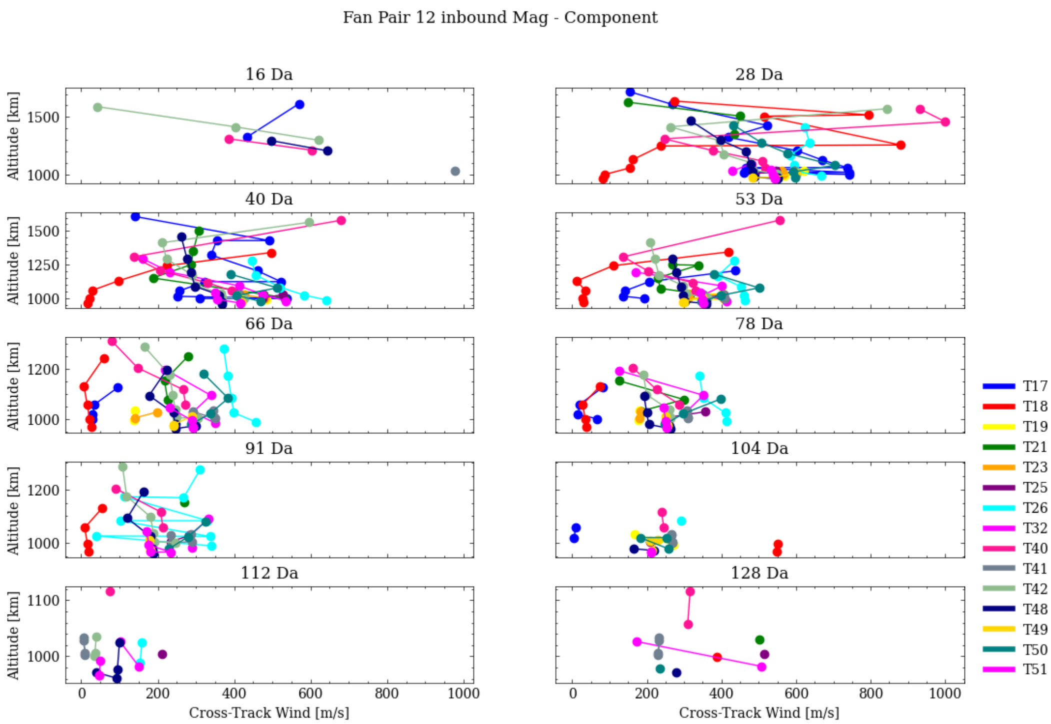

Figure 9. Derived cross-track ion velocities from the crossed-fan technique and the CAPS-IBS ion measurements. Each mass group is labeled with a mass number in the middle of the grouping in Daltons and several flybys are shown.

is likely simply due to the lighter masses being easier to accelerate in the upper atmosphere.

2.3 CAPS-IBS Ion Acceleration Measurements

In addition to the crossed-fan CAPS-IBS measurements and INMS low-energy ion velocity measurements we also look to unique measurements of ion velocity changes during the inbound and outbound legs of a few Cassini flybys that show clear signs of ion acceleration.

Figure 10 shows the direct connection of multiple ion species from a thermal distribution dominated by the velocity of the Cassini spacecraft (6 km/s) through the ionosphere to an accelerated flow with a velocity over 20 km/s or roughly 20% of the corotational velocity of 100 km/s. This observation is crucial as it shows the direct link between the thermal ions in the ionosphere and their accelerated counterparts further downstream and also show that some of Titan's complex chemistry will be accelerated away from the ionosphere.

One key observation pointed out in Figure 10 is that the acceleration is mass dependent with lighter masses being accelerated to greater velocities than heavier masses. In the figure we see that the peak for a group of ions roughly of mass 16 is accelerated from roughly 7 km/s to 20.5 km/s from 1400 km to 2100 km altitude. The ions that are roughly mass 28 are clearly seen with the same 7 km/s velocity near 1400 km, but at the 2100 km their peak energy is roughly 42 eV indicating a velocity of 17 km/s which is significantly less than the lighter components (note that if they had the same velocity the peak would appear at 61 eV).

3 Discussion and Conclusions

Here we presented several unique measurements of Titan's upper atmospheric ions and their velocities as observed by the Cassini INMS and CAPS instruments. These unique observations show a complex picture of the messy interaction of Saturn's magnetosphere with Titan's ionosphere. As has been simulated by many authors, this exposed ionosphere clearly has a complex interaction resulting in the acceleration of ionospheric components into the broader magnetosphere.

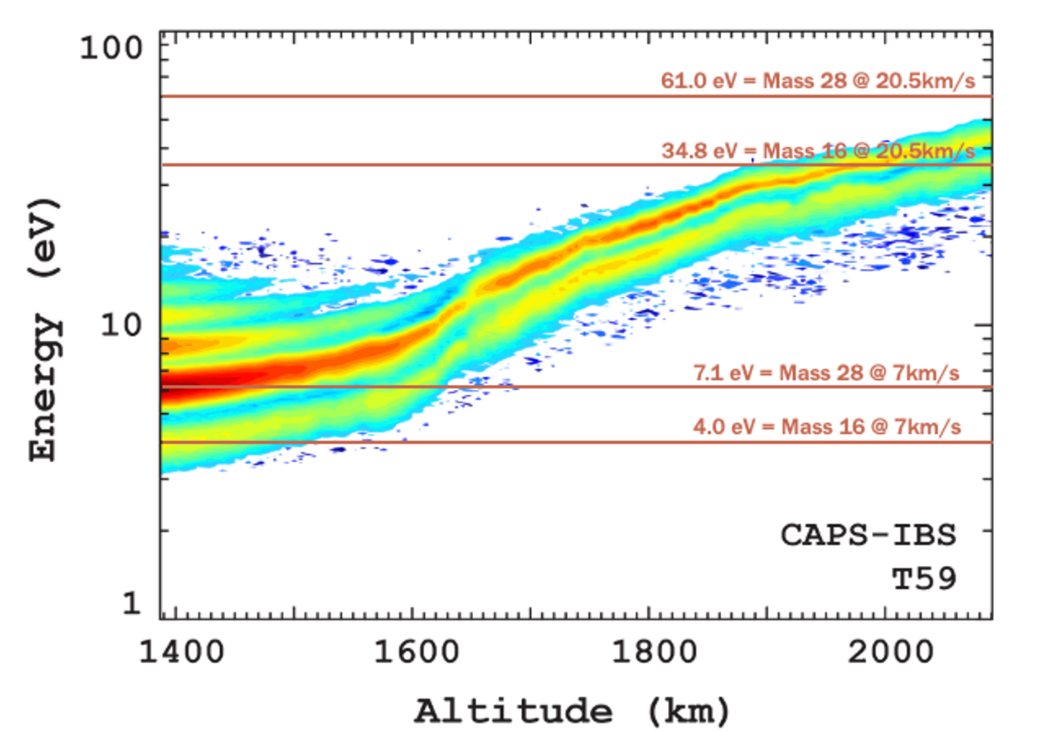

Figure 10. CAPS-IBS Observations from the T59 Titan flyby (24 July 2009) showing the direct acceleration of multiple species of ions from the upper atmosphere. The vertical axis is the measured energy from the CAPS-IBS instrument without the spacecraft velocity subtracted. The horizontal lines show the peak energies and velocities at 1400 km for two ion species groups and where they would appear at 2100 km if the acceleration were mass independent.

Our INMS and CAPS observations showed that heavy ions are being accelerated from Titan's ionosphere and that there are likely multiple processes responsible for this acceleration. The mass dependence of the observations of ion acceleration and the cross-track ion velocities seem to indicate some thermal process that has a mass-dependent term. However, a few observations shows mass independent acceleration likely due to the exposure to an electric field such as the convection electric field that would be present for the flowing plasma over Titan's exposed ionosphere.

These heavy ions appear to come from the second and third mass groupings in Titan's ionosphere containing complex hydrocarbons such as protonated methane (CH_5^+) and hydrogen cyanide ($HCNH^+$). These ions, once accelerated could escape the interaction and become a part of the magnetospheric flow. With this heavy flow, these ions likely don't remain in Saturn's magnetosphere for long and haven't been a major contributor to the ions seen in the inner magnetosphere. These are likely lost to interplanetary space due to the continual exposure of Titan's orbit to Saturn's magnetosheath and the solar wind.

4 Open Research

All data used in this paper is available from the Planetary Data System and is archived along with the Cassini archive. Note to reviewer - we are working the process to gain release approval to place the codes and data on GitHub as well as to put in place a Zenodo record of the data as well as the DOI of this data. We expect this process to complete before the review timeline and are therefore submitting this paper and will add in the open research details during the review cycle.

Acknowledgments

This work was funded by grant 80NSSC20K0378 from the NASA Cassini Data Analysis program.

References

Bame, S. J., Asbridge, J. R., Felthauser, H. E., Glore, J. P., Paschmann, G., Hemmerich, P., ... Rosenbauer, H. (1978). ISEE-1 and ISEE-2 Fast Plasma Experiment and the ISEE-1 Solar Wind Experiment. *IEEE Transactions on Geoscience Electronics*, *16*(3), 216–220. doi: 10.1109/TGE.1978.294550

Bell, J. M., Hunter Waite, J., Westlake, J. H., Bougher, S. W., Ridley, A. J., Perryman, R., & Mandt, K. (2014, 6). Developing a self-consistent description of Titan's upper atmosphere without hydrodynamic escape. *Journal of Geophysical Research: Space Physics*, *119*(6), 4957–4972. Retrieved from `https://onlinelibrary.wiley.com/doi/full/10.1002/2014JA019781https://onlinelibrary.wiley.com/doi/abs/10.1002/2014JA019781https://agupubs.onlinelibrary.wiley.com/doi/10.1002/2014JA019781` doi: 10.1002/2014JA019781

Coates, A. J., Crary, F. J., Lewis, G. R., Young, D. T., Waite, J. H., & Sittler, J. C. (2007, 11). Discovery of heavy negative ions in Titan's ionosphere. *Geophysical Research Letters*, *34*(22). Retrieved from `https://onlinelibrary.wiley.com/doi/full/10.1029/2007GL030978https://onlinelibrary.wiley.com/doi/abs/10.1029/2007GL030978https://agupubs.onlinelibrary.wiley.com/doi/10.1029/2007GL030978` doi: 10.1029/2007GL030978

Crary, F. J., Magee, B. A., Mandt, K., Waite, J. H., Westlake, J., & Young, D. T. (2009, 12). Heavy ions, temperatures and winds in Titan's ionosphere: Combined Cassini CAPS and INMS observations. *Planetary and Space Science*, *57*(14-15), 1847–1856. doi: 10.1016/J.PSS.2009.09.006

Cravens, T. E., Lindgren, C. J., & Ledvina, S. A. (1998, 10). A two-dimensional multifluid MHD model of Titans plasma environment. *Planetary and Space Science*, *46*(9-10), 1193–1205. doi: 10.1016/S0032-0633(98)00051-8

Hartle, R. E., Sittler, E. C., Ogilvie, K. W., Scudder, J. D., Lazarus, A. J., & Atreya, S. K. (1982, 3). Titan's ion exosphere observed from Voyager 1. *Journal of Geophysical Research: Space Physics*, *87*(A3), 1383–1394. Retrieved from `https://onlinelibrary.wiley.com/doi/full/10.1029/JA087iA03p01383https://onlinelibrary.wiley.com/doi/abs/10.1029/JA087iA03p01383https://agupubs.onlinelibrary.wiley.com/doi/10.1029/JA087iA03p01383` doi: 10.1029/JA087IA03P01383

Jiang, F. Y., Cui, J., Xu, J. Y., & Wei, Y. (2019, 5). Species-dependent ion escape on Titan. *Earth and Planetary Physics*, *3*(3), 183–189. Retrieved from `https://onlinelibrary.wiley.com/doi/full/10.26464/epp2019020https://onlinelibrary.wiley.com/doi/abs/10.26464/`

epp2019020https://agupubs.onlinelibrary.wiley.com/doi/10.26464/epp2019020 doi: 10.26464/EPP2019020

Ma, Y. J., Nagy, A. F., Cravens, T. E., Sokolov, I. V., Clark, J., & Hansen, K. C. (2004, 11). 3-D global MHD model prediction for the first close flyby of Titan by Cassini. *Geophysical Research Letters*, *31*(22), 1–4. Retrieved from https://onlinelibrary.wiley.com/doi/full/10.1029/2004GL021215https://onlinelibrary.wiley.com/doi/abs/10.1029/2004GL021215https://agupubs.onlinelibrary.wiley.com/doi/10.1029/2004GL021215 doi: 10.1029/2004GL021215

Mandt, K. E., Gell, D. A., Perry, M., Hunter Waite, J., Crary, F. A., Young, D., ... Liang, M. C. (2012, 10). Ion densities and composition of Titan's upper atmosphere derived from the Cassini Ion Neutral Mass Spectrometer: Analysis methods and comparison of measured ion densities to photochemical model simulations. *Journal of Geophysical Research: Planets*, *117*(E10). Retrieved from https://onlinelibrary.wiley.com/doi/full/10.1029/2012JE004139https://onlinelibrary.wiley.com/doi/abs/10.1029/2012JE004139https://agupubs.onlinelibrary.wiley.com/doi/10.1029/2012JE004139 doi: 10.1029/2012JE004139

Regoli, L. H., Coates, A. J., Thomsen, M. F., Jones, G. H., Roussos, E., Waite, J. H., ... Cox, G. (2016, 9). Survey of pickup ion signatures in the vicinity of Titan using CAPS/IMS. *Journal of Geophysical Research: Space Physics*, *121*(9), 8317–8328. Retrieved from https://onlinelibrary.wiley.com/doi/full/10.1002/2016JA022617https://onlinelibrary.wiley.com/doi/abs/10.1002/2016JA022617https://agupubs.onlinelibrary.wiley.com/doi/10.1002/2016JA022617 doi: 10.1002/2016JA022617

Romanelli, N., Modolo, R., Dubinin, E., Berthelier, J. J., Bertucci, C., Wahlund, J. E., ... Dougherty, M. (2014, 12). Outflow and plasma acceleration in Titan's induced magnetotail: Evidence of magnetic tension forces. *Journal of Geophysical Research: Space Physics*, *119*(12), 9992–10. Retrieved from https://onlinelibrary.wiley.com/doi/full/10.1002/2014JA020391https://onlinelibrary.wiley.com/doi/abs/10.1002/2014JA020391https://agupubs.onlinelibrary.wiley.com/doi/10.1002/2014JA020391 doi: 10.1002/2014JA020391

Sittler, E. C., Hartle, R. E., Viñas, A. F., Johnson, R. E., Smith, H. T., & Mueller-Wodarg, I. (2005, 9). Titan interaction with Saturn's magnetosphere: Voyager 1 results revisited. *Journal of Geophysical Research: Space Physics*, *110*(A9), 9302. Retrieved from https://onlinelibrary.wiley.com/doi/full/10.1029/2004JA010759https://onlinelibrary.wiley.com/doi/abs/10.1029/2004JA010759https://agupubs.onlinelibrary.wiley.com/doi/10.1029/2004JA010759 doi: 10.1029/2004JA010759

Strobel, D. F. (2009, 8). Titan's hydrodynamically escaping atmosphere: Escape rates and the structure of the exobase region. *Icarus*, *202*(2), 632–641. doi: 10.1016/J.ICARUS.2009.03.007

Vuitton, V., Yelle, R., & Lavvas, P. (2008, 11). Composition and chemistry of Titan's thermosphere and ionosphere. *Philosophical Transactions of the Royal Society A: Mathematical, Physical and Engineering Sciences*, *367*(1889), 729–741. Retrieved from https://royalsocietypublishing.org/doi/10.1098/rsta.2008.0233 doi: 10.1098/RSTA.2008.0233

Waite, J. H., Lewis, W. S., Kasprzak, W. T., Anicich, V. G., Block, B. P., Cravens, T. E., … Yelle, R. V. (2004, 12). The Cassini Ion and Neutral Mass Spectrometer (INMS) Investigation. *Space Science Reviews 2004 114:1*, *114*(1), 113–231. Retrieved from https://link.springer.com/article/10.1007/s11214-004-1408-2 doi: 10.1007/S11214-004-1408-2

Waite, J. H., Young, D. T., Cravens, T. E., Coates, A. J., Crary, F. J., Magee, B., & Westlake, J. (2007, 5). Planetary science: The process of tholin formation in Titan's upper atmosphere. *Science*, *316*(5826), 870–875. Retrieved from https://www.science.org/doi/10.1126/science.1139727 doi: 10.1126/SCIENCE.1139727/ASSET/653EF5D8-9D3F-41B2-AA03-AAE536691745/ASSETS/GRAPHIC/316{_}870{_}F4.JPEG

Westlake, J. H., Cravens, T. E., Johnson, R. E., Ledvina, S. A., Luhmann, J. G., Mitchell, D. G., … Woodson, A. K. (2016, 10). Titan's Interaction with Saturn's Magnetosphere. *Geophysical Monograph*, *222*, 291–305. Retrieved from https://onlinelibrary.wiley.com/doi/full/10.1002/9781119066880.ch23https://onlinelibrary.wiley.com/doi/abs/10.1002/9781119066880.ch23https://agupubs.onlinelibrary.wiley.com/doi/10.1002/9781119066880.ch23 doi: 10.1002/9781119066880.CH23

Westlake, J. H., Paranicas, C. P., Cravens, T. E., Luhmann, J. G., Mandt, K. E., Smith, H. T., ... Wahlund, J. E. (2012, 10). The observed composition of ions outflowing from Titan. *Geophysical Research Letters*, *39*(19), 19104. Retrieved from https://onlinelibrary.wiley.com/doi/full/10.1029/2012GL053079https://onlinelibrary.wiley.com/doi/abs/10.1029/2012GL053079https://agupubs.onlinelibrary.wiley.com/doi/10.1029/2012GL053079 doi: 10.1029/2012GL053079

Young, D. T., Barraclough, B. L., Berthelier, J. J., Blanc, M., Burch, J. L., Coates, A. J., ... Kelha, V. (1996). Cassini plasma spectrometer investigation. *Proceedings of SPIE - The International Society for Optical Engineering*, *2803*, 118–128. Retrieved from https://link.springer.com/chapter/10.1007/978-1-4020-2774-1_1 doi: 10.1007/978-1-4020-2774-1{_}1/COVER

Figure 1.

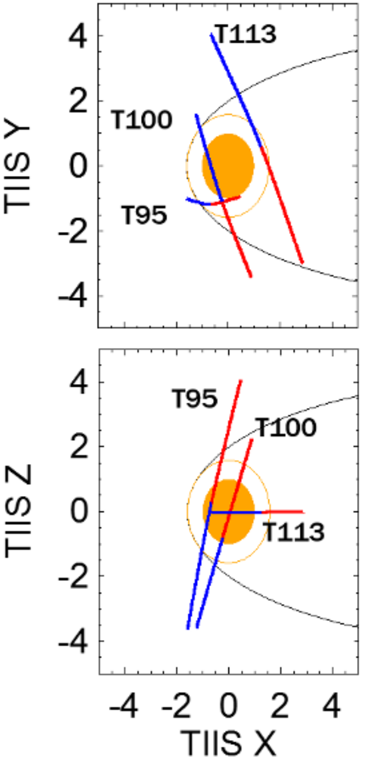

T113
T100
T95
TIIS Y
4
2
0
-2
-4
T95
T100
T113
TIIS Z
4
2
0
-2
-4
-4
-2
0
2
4
TIIS X

Figure 2.

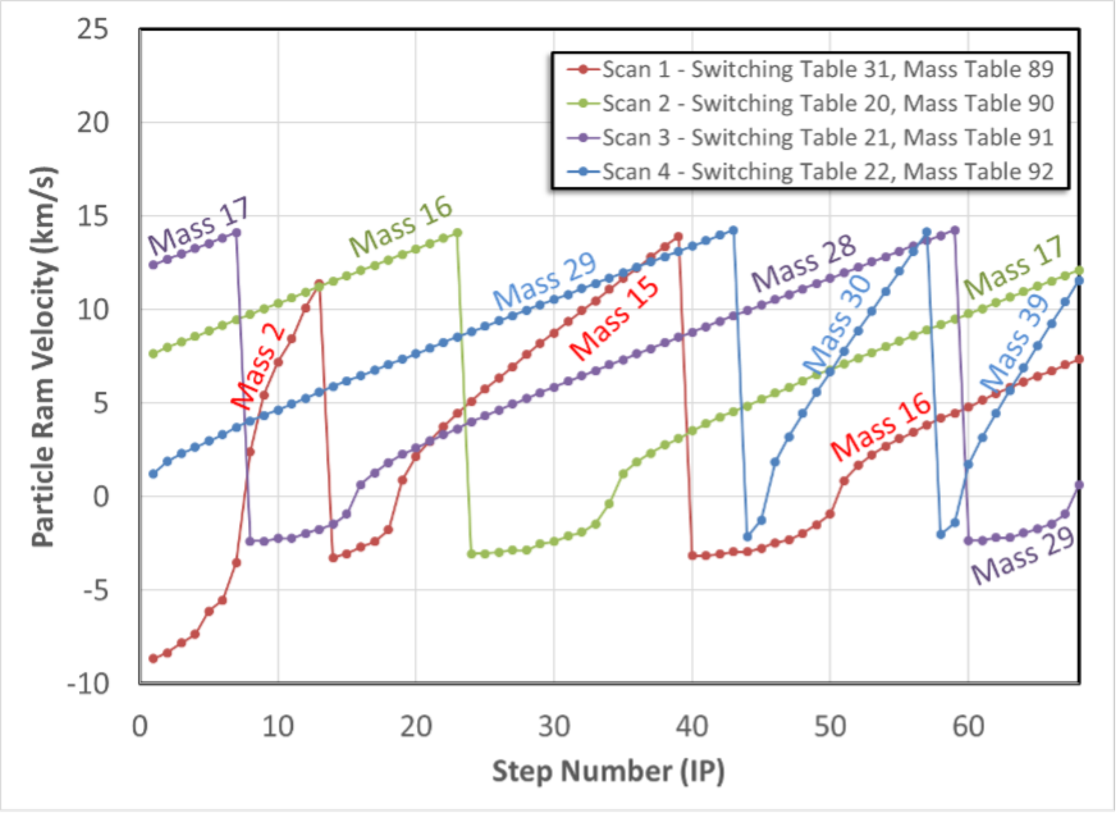

Scan 1 - Switching Table 31, Mass Table 89
Scan 2 - Switching Table 20, Mass Table 90
Scan 3 - Switching Table 21, Mass Table 91
Scan 4 - Switching Table 22, Mass Table 92
Mass 17
Mass 16
Mass 2
Mass 29
Mass 15
Mass 28
Mass 30
Mass 17
Mass 39
Mass 16
Mass 29
Particle Ram Velocity (km/s)
Step Number (IP)
25
20
15
10
5
0
-5
-10
0
10
20
30
40
50
60

Figure 3.

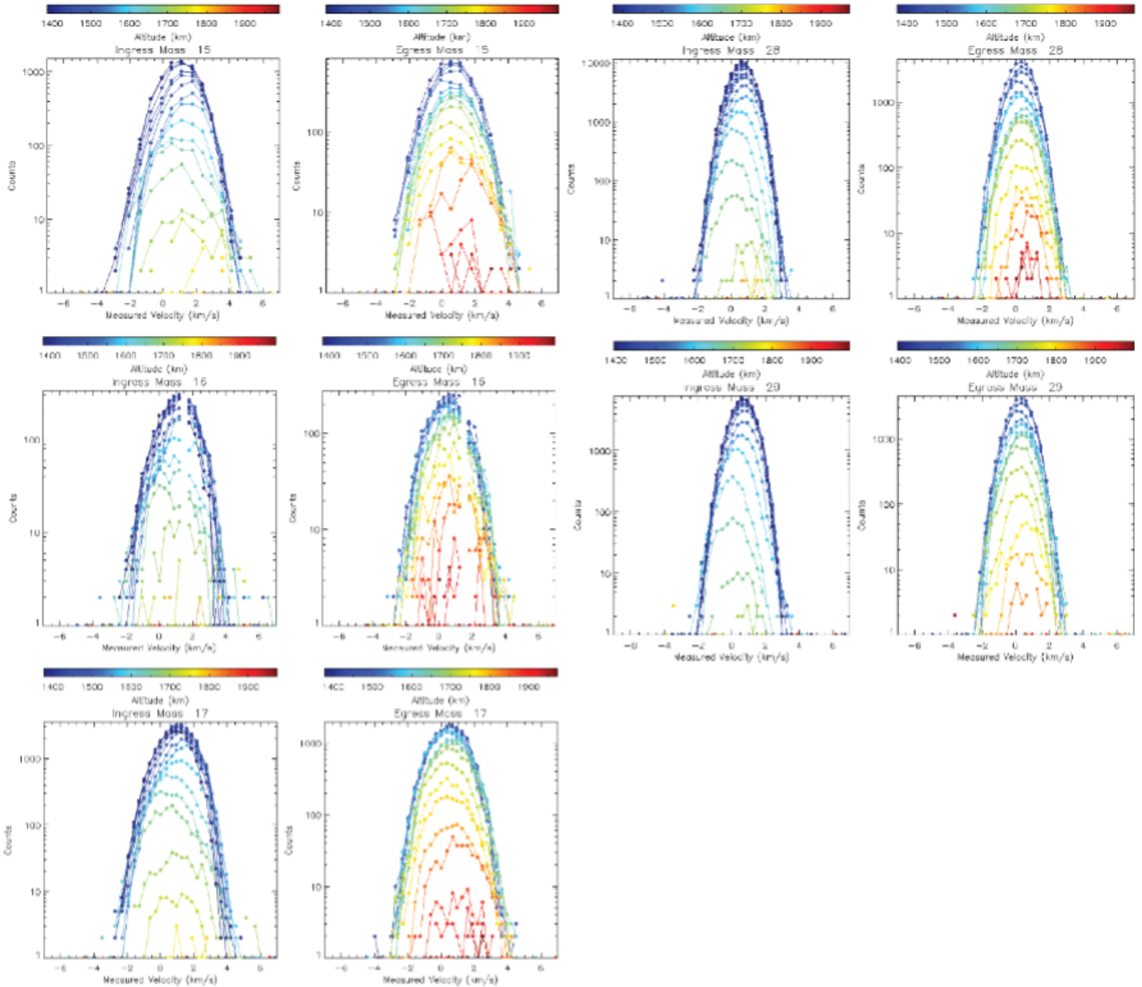
Altitude (km)
Ingress Mass 15
Egress Mass 15
Ingress Mass 28
Egress Mass 28
Ingress Mass 16
Egress Mass 16
Ingress Mass 29
Egress Mass 29
Ingress Mass 17
Egress Mass 17
Counts
Measured Velocity (km/s)

Figure 4.

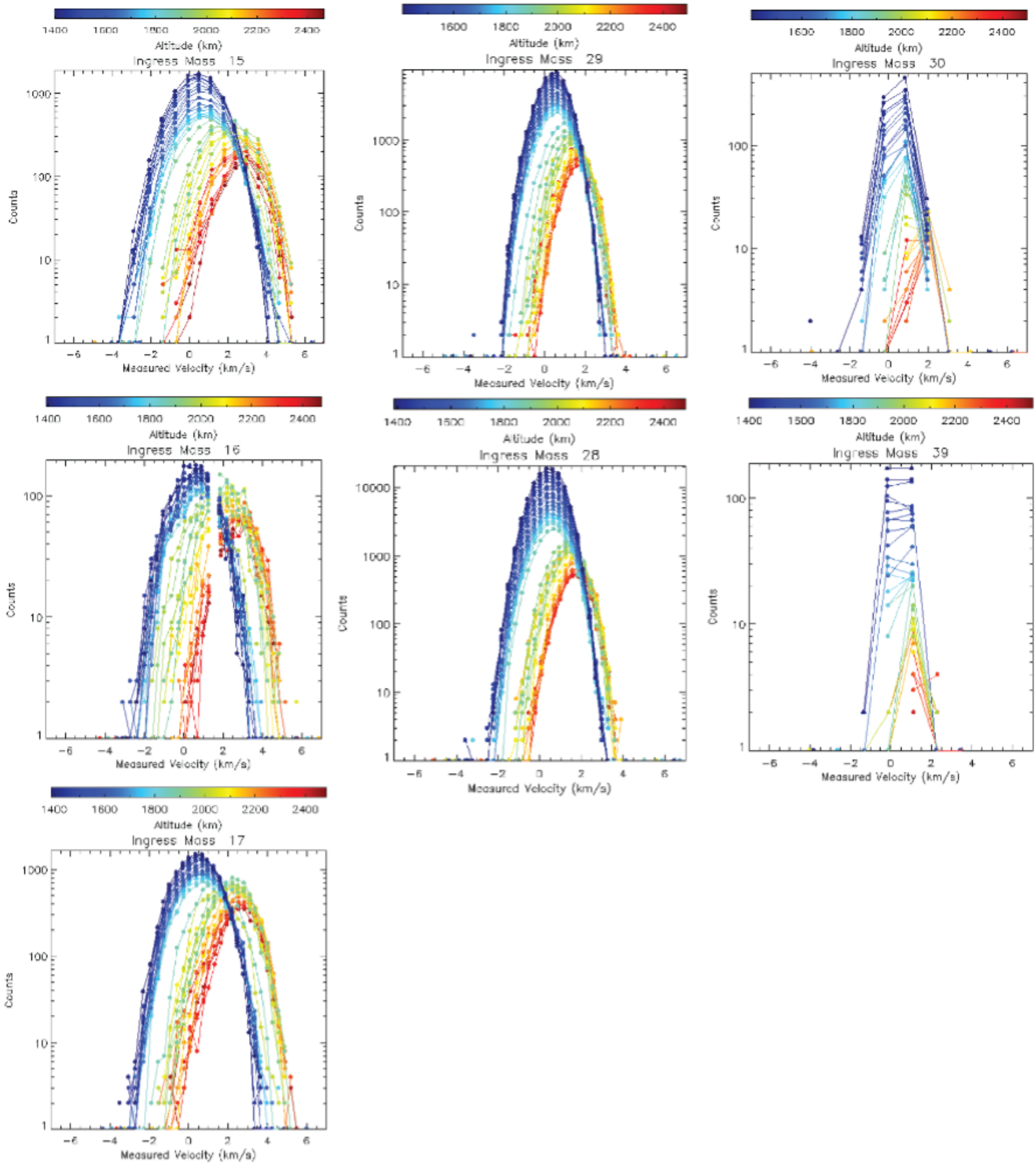

Altitude (km)
Ingress Mass 15
Counts
Measured Velocity (km/s)
Altitude (km)
Ingress Mass 29
Counts
Measured Velocity (km/s)
Altitude (km)
Ingress Mass 30
Counts
Measured Velocity (km/s)
Altitude (km)
Ingress Mass 16
Counts
Measured Velocity (km/s)
Altitude (km)
Ingress Mass 28
Counts
Measured Velocity (km/s)
Altitude (km)
Ingress Mass 39
Counts
Measured Velocity (km/s)
Altitude (km)
Ingress Mass 17
Counts
Measured Velocity (km/s)

Figure 5.

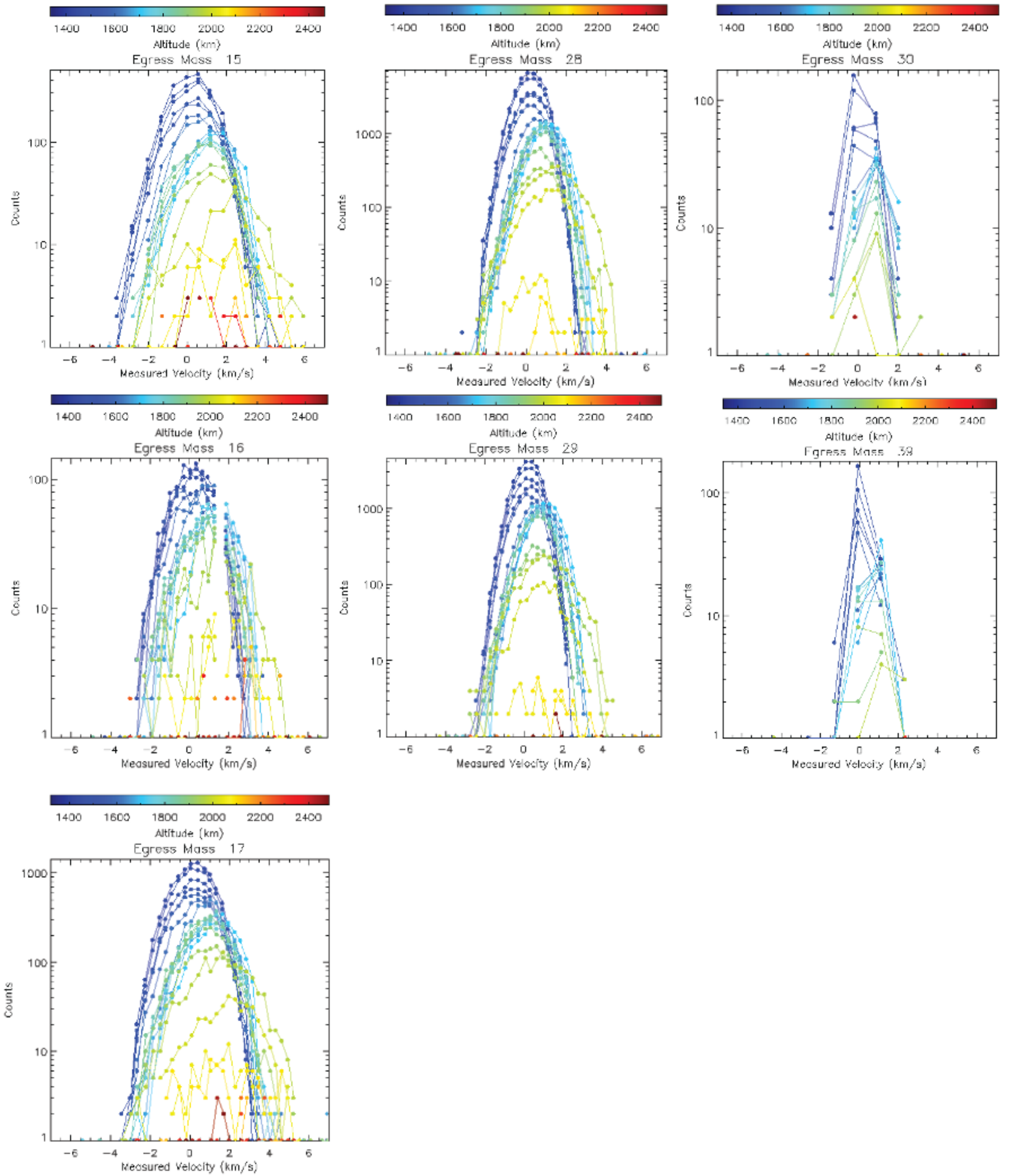

Altitude (km)
1400 1600 1800 2000 2200 2400
Egress Mass 15
Egress Mass 28
Egress Mass 30
Egress Mass 16
Egress Mass 29
Egress Mass 39
Egress Mass 17
Counts
Measured Velocity (km/s)

Figure 6.

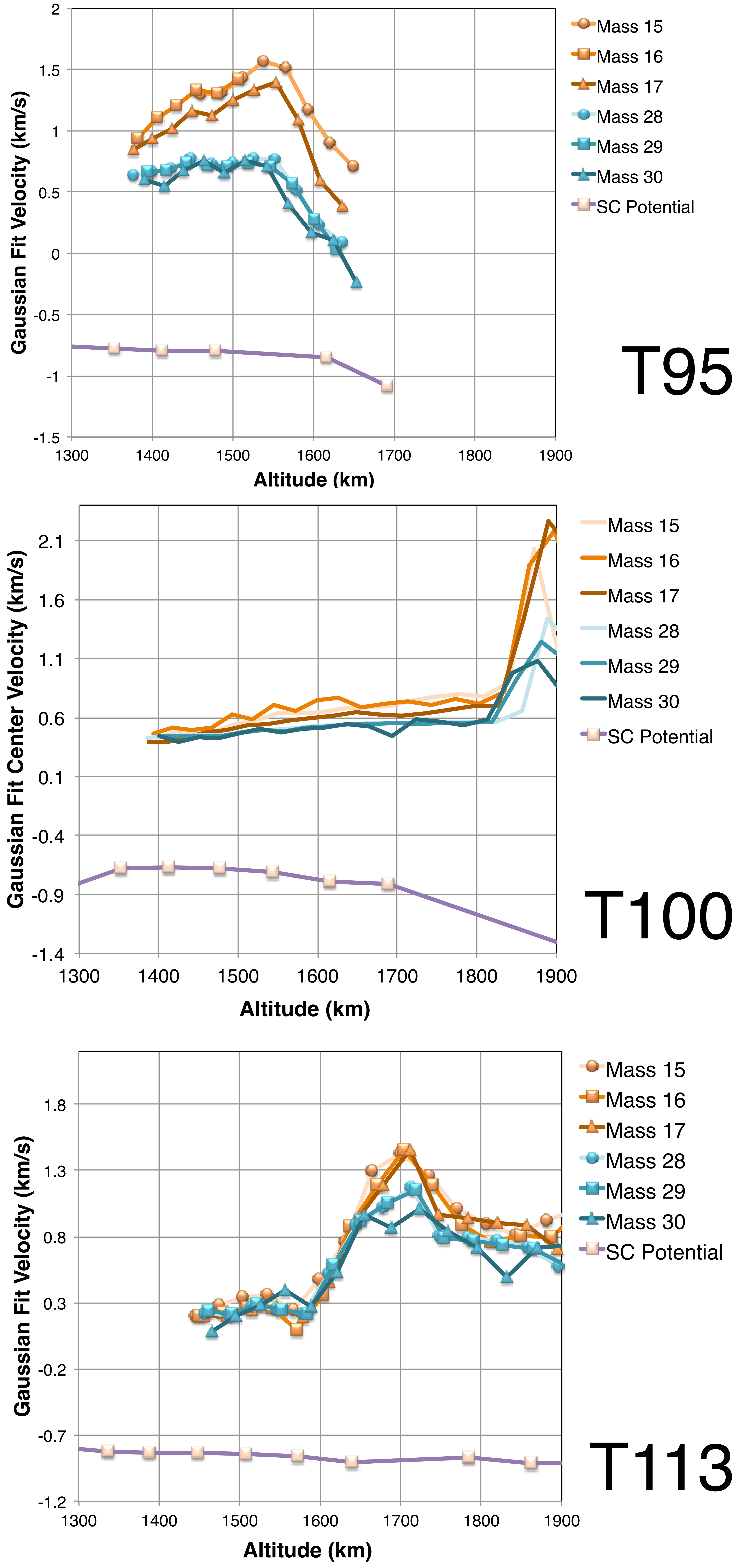

Gaussian Fit Velocity (km/s)
Altitude (km)
Mass 15
Mass 16
Mass 17
Mass 28
Mass 29
Mass 30
SC Potential
T95
Gaussian Fit Center Velocity (km/s)
Altitude (km)
Mass 15
Mass 16
Mass 17
Mass 28
Mass 29
Mass 30
SC Potential
T100
Gaussian Fit Velocity (km/s)
Altitude (km)
Mass 15
Mass 16
Mass 17
Mass 28
Mass 29
Mass 30
SC Potential
T113

Figure 7.

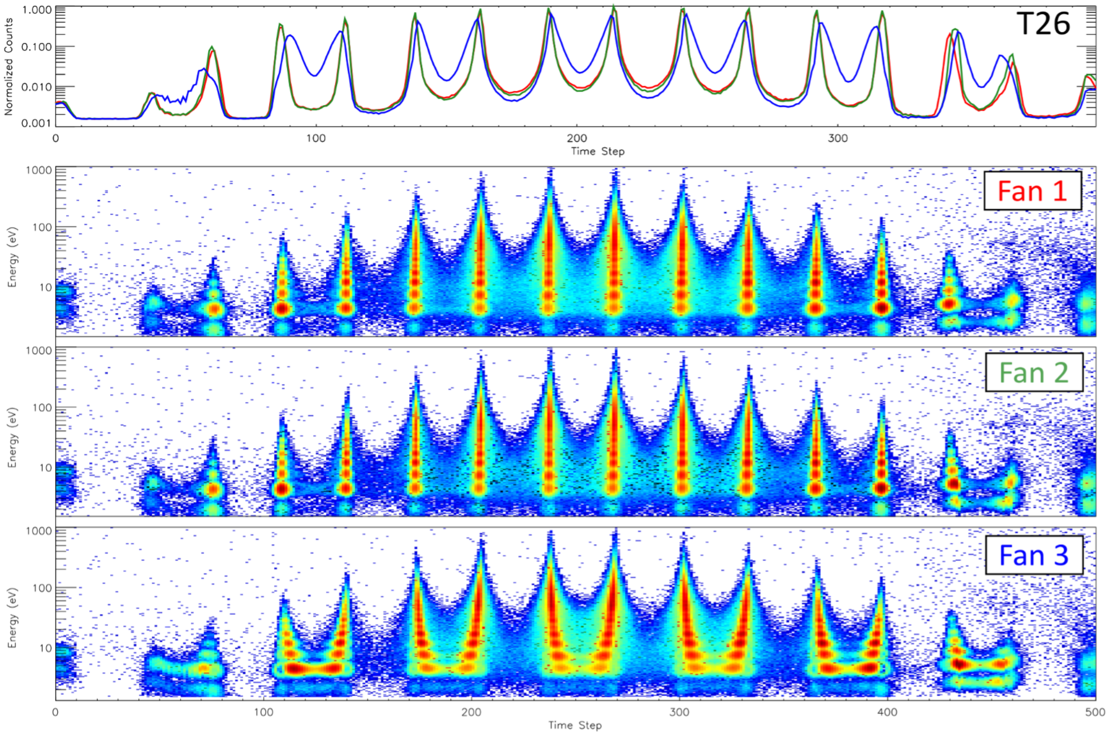

T26
Normalized Counts
1.000
0.100
0.010
0.001
0
100
200
300
Time Step
Fan 1
Fan 2
Fan 3
Energy (eV)
1000
100
10
0
100
200
300
400
500
Time Step

Figure 8.

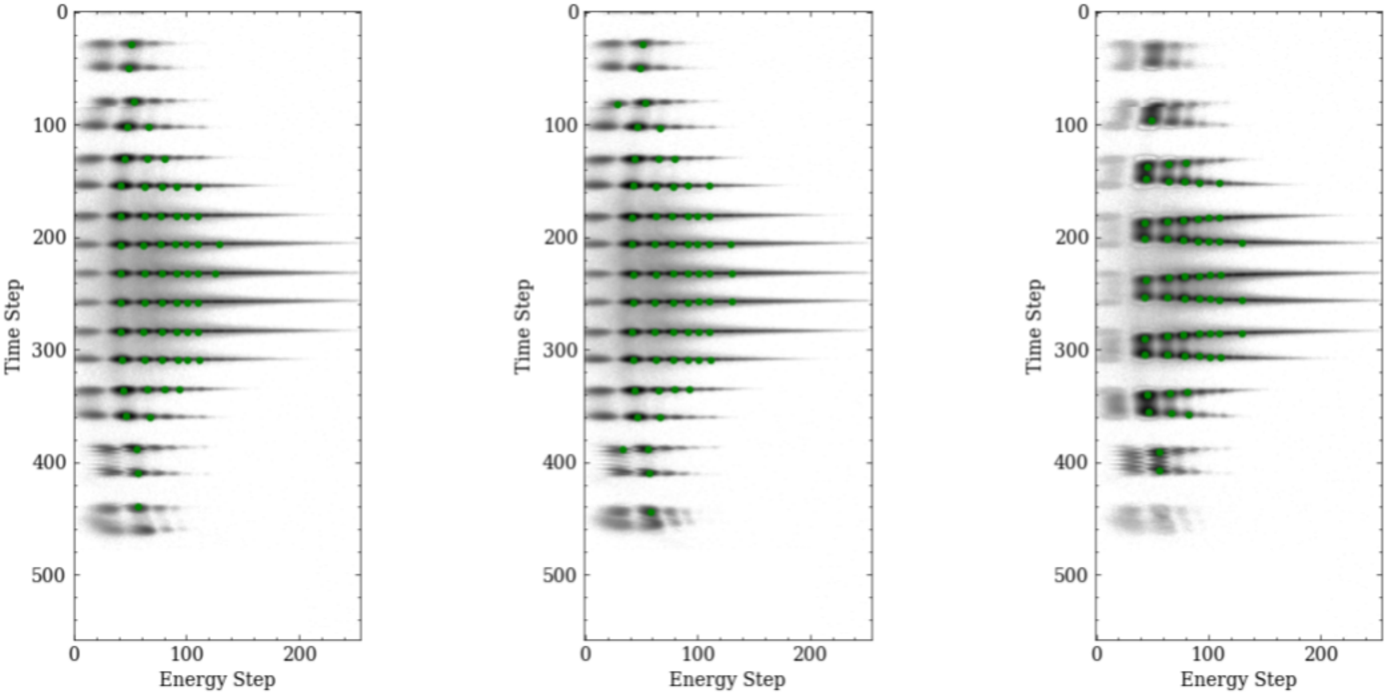

Time Step
Energy Step
0
100
200
300
400
500
0
100
200
Time Step
Energy Step
Time Step
Energy Step

Figure_8_fixed_scpot.png. Figure_8_fixed_scpot.png

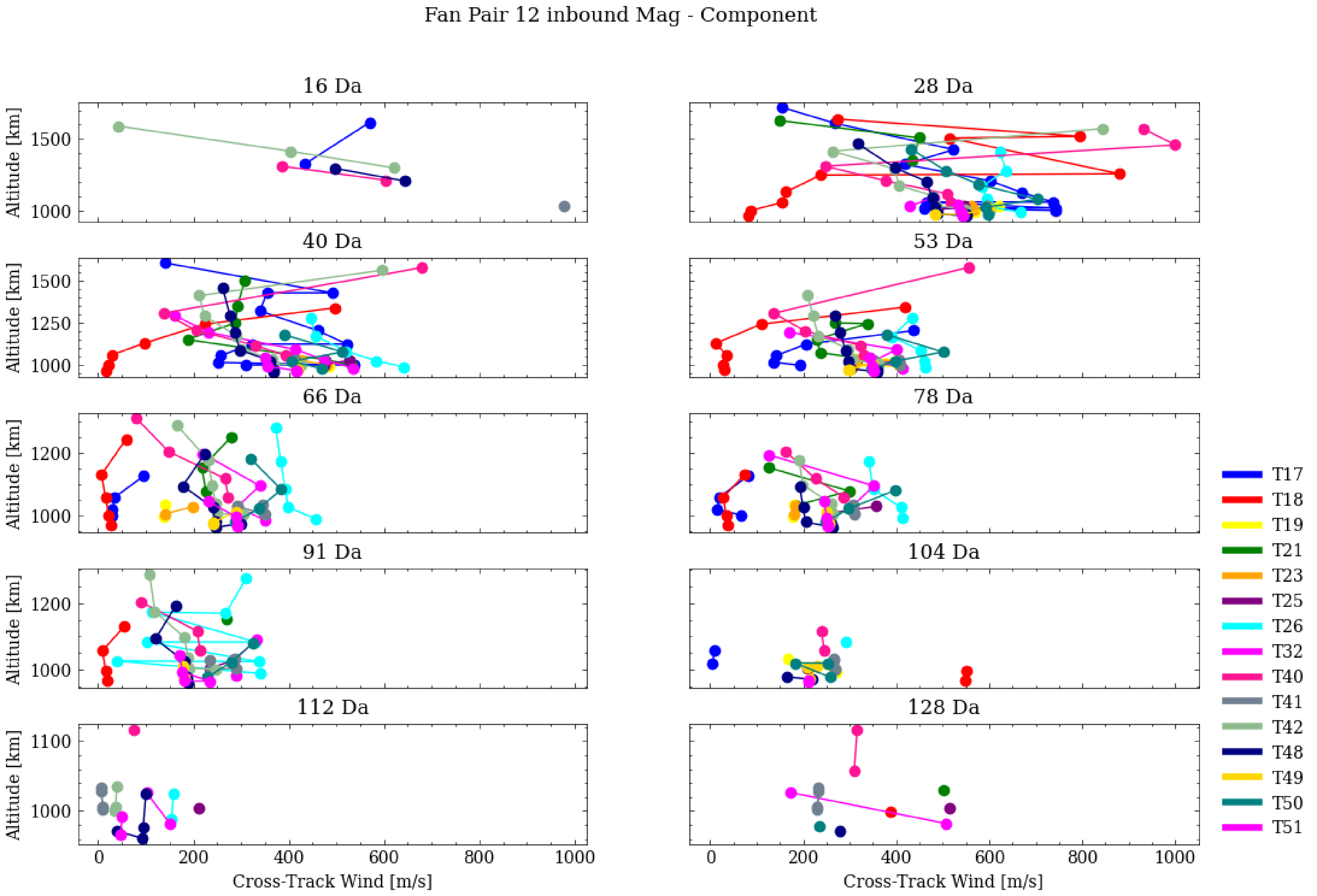
Fan Pair 12 inbound Mag - Component
16 Da
28 Da
40 Da
53 Da
66 Da
78 Da
91 Da
104 Da
112 Da
128 Da
Altitude [km]
Cross-Track Wind [m/s]
T17
T18
T19
T21
T23
T25
T26
T32
T40
T41
T42
T48
T49
T50
T51

T59-Accleration.png. T59-Accleration.png

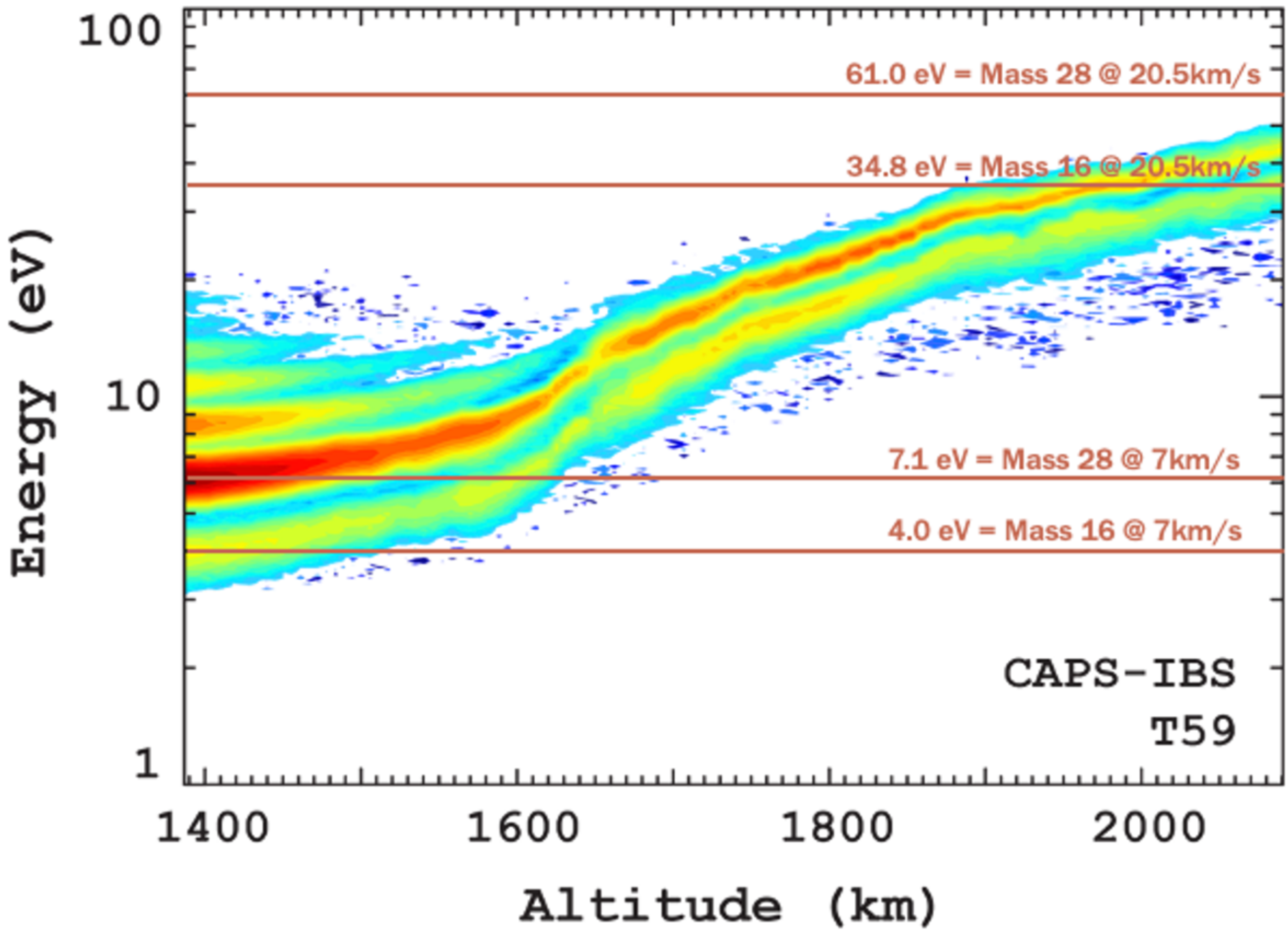

61.0 eV = Mass 28 @ 20.5km/s
34.8 eV = Mass 16 @ 20.5km/s
7.1 eV = Mass 28 @ 7km/s
4.0 eV = Mass 16 @ 7km/s
CAPS-IBS
T59
Energy (eV)
100
10
1
1400
1600
1800
2000
Altitude (km)